Pair-correlation functions for partially ionized hydrogen*

M. A. Pokrant and A. A. Broyles
Department of Physics and Astronomy, University of Florida, Gainesville, Florida 32611

Tucson Dunn
Department of Physics, Louisiana Tech University, Ruston, Louisiana 71270

(Received 6 February 1974)

A method is presented for calculating the pair-correlation functions for a high-density quantum-mechanical plasma of protons and electrons. The Slater sum is approximated in the form of a classical Boltzmann factor with the Coulomb potentials replaced by effective potentials. The effective potentials contain the classical potential plus quantum corrections. The quantum effects may be separated into symmetry effects, diffraction effects, and coupling between the two. This method is exact at infinite temperatures and is tested here down to temperatures at which there is about 40% ionization. The pair-correlation functions are obtained from a Monte Carlo calculation. The fraction of electrons in the ground state of an atom is also calculated; an approximate formula for this fraction is $(1/2)[1-\mathrm{erf}(b \ln T/T_0)]$, where b and T_0 are simple fitted functions of the density.

I. INTRODUCTION

The fact that quantum-mechanical effects would have to be included in the calculation of thermodynamic properties of a dense plasma was realized more than 40 years ago. Uhlenbeck and Gropper[1] formulated the problem in 1932. It was clear that the short-range classical Coulomb divergence for the proton-electron interaction would have to be eliminated by including the quantum-mechanical effects. Many authors[2-25] have treated this problem using a variety of approaches. While Kirkwood[3] was the first to have suggested the use of an "effective" potential between charged particles as a means of including quantum effects, Morita[5] would appear to have been the first to apply the idea. Ebeling and coworkers[10,11] have made considerable progress on the problem. They have made assumptions which kept most of their calculations analytic. Storer and Davies[17,18] and Barker[20-22] have developed methods for the exact evaluation of effective potentials in the low-density limit. Dunn and Broyles[23] developed a technique for including the density dependence of the effective potentials. This method was applied to the electron gas and was later extended to a hydrogen plasma.[25] This paper will apply the same general method to hydrogen and will investigate whether or not this method, which was developed for plasmas, can be extended to a system which is not completely ionized.

Since hydrogen is completely ionized at very high temperatures, it is desirable to take the nuclei (protons) and electrons as the constituent particles in any theoretical treatment. As the temperature is lowered, some electrons will combine with the protons to form atoms and ions as new particles. The number of these particles will be subject to fluctuation, since they will be continually forming and breaking up. But the most serious difficulty arises in the determination of the potentials that act between these atoms, ions, nuclei, and electrons. Conceptually, the simplest procedure is to continue to treat the systems as nuclei and electrons. Then the interaction potential is known to be the Coulomb potential. If properly handled, these electrons will associate with the nuclei in such a manner as to form the proper number of atoms and ions.

A first step in this direction was presented in Ref. 25. In this paper, we will present a modified derivation of the method of Ref. 25, improving the approximations. Distribution functions and ionization curves for hydrogen at several densities will be presented.

In order to obtain distribution functions, it is necessary to evaluate multidimensional integrals over the Slater sum

$$W(r_1, \ldots, r_N) = c \sum_n \Psi_n^* e^{-\beta E_n} \Psi_n , \tag{1.1}$$

where

$$c = \prod N_\nu ! \lambda_\nu^{3N_\nu} , \tag{1.2}$$

$$\lambda_\nu^2 = 4\pi\alpha_\nu\beta, \quad \alpha_\nu = \hbar^2/2m_\nu, \quad \beta = 1/kT. \tag{1.3}$$

In these equations, N_ν is the number of particles of the νth kind, each having a mass m_ν. The wave function is a properly symmetrized eigenfunction for the entire macroscopic system with eigenvalue E_n, where n represents a complete set of quantum numbers.

One may write

$$W = e^{-B} \tag{1.4}$$

and expand B in terms of two-body functions, three-body functions, etc.:

$$B \simeq \sum_{i<j} w_{ij} + \sum_{i<j<k} w^{(3)}_{ijk} + \cdots . \tag{1.5}$$

In the limit of infinite temperature, the Slater sum [Eq. (1.1)] goes over to the classical Boltzmann factor

$$W \xrightarrow[T\to\infty]{} \exp(-\sum_{i<j} \beta v_{ij}) , \tag{1.6}$$

where v_{ij} is the classical Coulomb potential. Thus the logical first step in using the expansion in Eq. (1.5) is to truncate the series after the first term:

$$B \simeq \sum_{i<j} w_{ij} . \tag{1.7}$$

One of the purposes of this investigation is to determine where this approximation is valid. In the limit of infinite temperature,

$$w_{ij} \xrightarrow[T\to\infty]{} \beta v_{ij} . \tag{1.8}$$

The problem is then to determine how w differs from βv at finite temperatures. A method for determining w is presented in Sec. II.

The effective potentials are illustrated in Sec. III. Distribution functions can be computed by integrating the Slater sum over all but two, three, etc., particles. Because of the way in which we have approximated w, the distribution functions can be obtained by using one of the procedures which have been developed for the classical theory of fluids. Radial distribution functions obtained by a Monte Carlo[26-28] (MC) calculation are presented in Sec. IV.

II. DIFFERENTIAL EQUATIONS FOR THE EFFECTIVE POTENTIALS

In this section we shall derive equations for obtaining the effective pair potential for any system of nuclei and electrons interacting with Coulomb potentials. This result will be used to obtain the effective potentials for hydrogen in Sec. III.

Since the Slater sum is invariant under unitary transformations, the energy eigenfunctions in Eq. (1.1) may be replaced by any complete set of functions, provided that E_n is replaced by the Hamiltonian. Thus we may write

$$W = c \sum_n (e^{-\beta H/2}\Psi_n)^*(e^{-\beta H/2}\Psi_n) . \tag{2.1}$$

The Hamiltonian is

$$H = -\Box^2 + V , \tag{2.2}$$

where $\Box$ is a $3N$-dimensional vector operator defined so that

$$\Box^2 = \sum_j \alpha_j \nabla_j^2, \quad \Box A \cdot \Box B = \sum_j \alpha_j \nabla_j A \cdot \nabla_j B \tag{2.3}$$

and the interaction potential V is

$$V = \sum_{i<j} v_{ij} = \sum_{i<j} Z_i Z_j e^2 / r_{ij} . \tag{2.4}$$

In order to obtain a differential equation, we differentiate the Slater sum with respect to β to obtain

$$\frac{\partial W}{\partial \beta} = \frac{3N}{2\beta} W - VW + \tfrac{1}{2} c \sum_n [(\Box^2 e^{-\beta H/2}\Psi_n)^*(e^{-\beta H/2}\Psi_n) + (e^{-\beta H/2}\Psi_n)^*(\Box^2 e^{-\beta H/2}\Psi_n)] . \tag{2.5}$$

Note that the terms in the brackets also occur in the expression

$$\Box^2 W = c \sum_n [(\Box^2 e^{-\beta H/2}\Psi_n)^*(e^{-\beta H/2}\Psi_n) + (e^{-\beta H/2}\Psi_n)^*(\Box^2 e^{-\beta H/2}\Psi_n)] + 2X , \tag{2.6}$$

where we have defined

$$X = c \sum_n (\Box e^{-\beta H/2}\Psi_n)^* \cdot (\Box e^{-\beta H/2}\Psi_n) . \tag{2.7}$$

Combining Eqs. (2.5) and (2.6), we obtain

$$\frac{\partial W}{\partial \beta} = \frac{3N}{2\beta} W - VW + \tfrac{1}{2}\Box^2 W - X . \tag{2.8}$$

By substituting $W = e^{-B}$ into Eq. (2.8), we obtain

$$\frac{\partial B}{\partial \beta} = V + \tfrac{1}{2}\Box^2 B - \tfrac{1}{4}\Box B \cdot \Box B + Y , \tag{2.9}$$

where

$$Y = X/W - 3N/2\beta - \tfrac{1}{4}\Box B \cdot \Box B \tag{2.10}$$

has been introduced for several reasons. First, this form of the equation will make the comparison with the method in Ref. 25 clear. Second, observe that if we replace Ψ_n by plane waves in Eqs. (2.1) and (2.8) and neglect the Coulomb potential in the Hamiltonian, then

$$X/W \to 3N/2\beta . \tag{2.11}$$

Furthermore, at extremely high temperatures where this replacement is most nearly valid, $B \simeq \beta V$. Hence, the last term in Eq. (2.10) goes to

zero, and we conclude that

$$Y \to 0 \text{ as } T \to \infty . \tag{2.12}$$

If, on the other hand, we replace the sum over n in Eqs. (2.1) and (2.8) by a single state, and let Ψ be a real energy eigenfunction, then $\Psi^2 \sim e^{-B}$. Hence, we have

$$X/W \to \tfrac{1}{4}\Box B \cdot \Box B . \tag{2.13}$$

Since this replacement would be valid at low temperatures where the ground state is dominant, we conclude that

$$Y \to 0 \text{ as } T \to 0 . \tag{2.14}$$

The above arguments can be made more rigorous by manipulating various equations of this section. In summary, we have taken three quantities, each of which is important in some temperature range, and combined them into a single quantity which is relatively small due to cancellation among the terms.

Exactly the same procedure used to derive Eq. (2.9), when applied to a mixture of independent ideal gases, yields

$$\frac{\partial B_I}{\partial \beta} = \tfrac{1}{2}\Box^2 B_I - \tfrac{1}{4}\Box B_I \cdot \Box B_I + Y_I . \tag{2.15}$$

Taking the difference of Eqs. (2.9) and (2.15) and defining

$$U = B - B_I , \tag{2.16}$$

we obtain

$$\frac{\partial U}{\partial \beta} = V + \tfrac{1}{2}\Box^2 U - \tfrac{1}{4}\Box U \cdot \Box U - \tfrac{1}{2}\Box U \cdot \Box B_I + Y - Y_I . \tag{2.17}$$

We will refer to B_I as the symmetry (or ideal gas) effective potential, U as the diffraction effective potential, and B as the total effective potential. Those effects due to the symmetry of the wave function required by Fermi or Bose statistics, which would be present even in a noninteracting system, are included in B_I. The effects of the classical potential, the diffraction effects due to the uncertainty principle, and the coupling between symmetry and diffraction effects are all contained in U.

At this stage we see that two major obstacles must be overcome. The function Y involving a summation over a complete set of wave functions must be evaluated. In addition, this many-body equation must be separated into equations involving only pairs of particles.

Lado[14] has shown that B_I may be approximated by

$$B_I \simeq \sum_{i<j} s_{ij} , \tag{2.18}$$

and he has given a method for computing s_{ij} for both Fermi and Bose ideal gases. In the numerical computations, we use the simpler procedure of inverting the hypernetted chain equation[29] to obtain s_{ij}.

Then, if we write

$$U = \sum_{i<j} u_{ij} , \tag{2.19}$$

the total effective pair potentials are given by

$$w_{ij} = u_{ij} + s_{ij} . \tag{2.20}$$

We will now obtain an equation for the diffraction pair potentials. In order to do this, it is necessary to use a pair approximation to $(Y - Y_I)$ so that

$$Y - Y_I \simeq \sum_{i<j} y_{ij} . \tag{2.21}$$

The quantity y_{ij} is taken to be $(Y - Y_I)$ for a two-particle system in which the Coulomb potential has been replaced by an average potential reflecting the effects of the other particles. A derivation of y_{ij} using Thomas-Fermi approximations is given in Appendix A.

By substituting Eqs. (2.18), (2.19), and (2.21) into Eq. (2.17), we obtain

$$\frac{1}{2}\sum_{i\neq j} D_{ij} + \frac{1}{2}\sum_{i\neq j}\sum_{k} T_{ijk} = 0 , \tag{2.22}$$

where

$$\begin{aligned} D_{ij} = &-\frac{\partial u_{ij}}{\partial \beta} + v_{ij} + \tfrac{1}{2}(\alpha_i + \alpha_j)\nabla_i^2 u_{ij} \\ &- \tfrac{1}{4}(\alpha_i + \alpha_j)\nabla_i u_{ij} \cdot \nabla_i u_{ij} \\ &- \tfrac{1}{2}(\alpha_i + \alpha_j)\nabla_i u_{ij} \cdot \nabla_i s_{ij} + y_{ij} ; \end{aligned} \tag{2.23}$$

$$\begin{aligned} T_{ijk} = &-\tfrac{1}{2}\alpha_k [\nabla_k u_{ik} \cdot \nabla_k u_{jk} \\ &+ \nabla_k u_{ik} \cdot \nabla_k s_{jk} + \nabla_k u_{jk} \cdot \nabla_k s_{ik}] . \end{aligned} \tag{2.24}$$

To obtain a solvable equation, the summations must be eliminated. To do this, multiply Eq. (2.22) by $e^{-i\vec{x}\cdot\vec{r}_{\mu\nu}}$ and integrate over $d\vec{r}_\mu d\vec{r}_\nu$. Some manipulations then give

$$\begin{aligned} \frac{\partial \tilde{u}_{\mu\nu}}{\partial \beta} = &\tilde{v}_{\mu\nu} - \tfrac{1}{2}(\epsilon_\mu + \epsilon_\nu)\tilde{u}_{\mu\nu} - \tilde{Q}_{\mu\nu} \\ &- \tfrac{1}{2}(\alpha_\mu + \alpha_\nu)(\nabla u_{\mu\nu} \cdot \nabla s_{\mu\nu})^F + \tilde{y}_{\mu\nu} \\ &- \frac{1}{2}\frac{1}{\Omega}\sum_k \epsilon_k(\tilde{u}_{\mu k}\tilde{u}_{\nu k} + \tilde{u}_{\mu k}\tilde{s}_{\nu k} + \tilde{u}_{\nu k}\tilde{s}_{\mu k}), \\ &x \neq 0 , \end{aligned} \tag{2.25}$$

where we have defined

$$\epsilon_\mu = \alpha_\mu x^2 \ , \tag{2.26}$$

$$Q_{\mu\nu}(r) = \tfrac{1}{4}(\alpha_\mu + \alpha_\nu)\nabla u_{\mu\nu}(r)\cdot\nabla u_{\mu\nu}(r) \ ; \tag{2.27}$$

both the tilde and the superscript F denote the Fourier transform

$$\tilde{u}(x) = \int u(r) e^{-i\vec{x}\cdot\vec{r}}\, d\vec{r} \ . \tag{2.28}$$

A comparison of Eq. (2.25) with Eq. (33) of Ref. 25 reveals that the difference in the two methods is that $y_{\mu\nu}$ was neglected in Ref. 25. As we shall see in Sec. III, including $y_{\mu\nu}$ gives significantly better results.

Under the assumption that $\tilde{u}_{\mu k}$ must be the same function for all particles k which are of the same type (e.g., nuclei), the last term in Eq. (2.25) may be simplified to

$$-\frac{1}{2}\sum_\eta \rho_\eta \epsilon_\eta \tilde{u}_{\mu\eta}\tilde{u}_{\nu\eta} - \tfrac{1}{2}\rho_\mu\epsilon_\mu\tilde{u}_{\mu\nu}\tilde{s}_{\mu\mu} - \tfrac{1}{2}\rho_\nu\epsilon_\nu\tilde{u}_{\mu\nu}\tilde{s}_{\nu\nu} \ ,$$

where the sum over η now denotes a sum over the types of particles. We have also utilized the fact that

$$\tilde{s}_{\mu\nu} = \tilde{s}_{\mu\mu}\delta_{\mu\nu} \ ,$$

since there is no symmetry interaction between particles of different types.

III. PAIR EFFECTIVE POTENTIALS

We will now apply Eq. (2.25) to hydrogen. Because the Hamiltonian does not contain the spin orientations of the particles, we may consider particles with different spin orientations to be of distinct types. Therefore we should consider four kinds of particles: spin-up protons, spin-down protons, spin-up electrons, and spin-down electrons. We assume equal numbers of each type of particle. Because only relatively high temperatures will be considered, the spin of the nuclei will be neglected. The problem may be further simplified by observing that the fourth term on the right-hand side of Eq. (2.25) only occurs in the equation for the diffraction potential for electrons with parallel spin. If we neglect this term, then the diffraction potentials between pairs of electrons with parallel and antiparallel spin are equal. Numerical calculations at low densities indicate that this is an excellent approximation. This does not mean that the total effective potentials are the same; the symmetry effective potential must still be included to get the total effective potential for electrons with parallel spin. It does indicate that the effects due to the spatial extent of the wave function (diffraction effects) on the effective potentials are nearly independent of the relative spin orientations of two interacting electrons. If we let 1 denote protons, 2 denote spin-up electrons, and 3 denote spin-down electrons, then the total effective pair potentials are given by

$$w_{11} = u_{11} \ , \tag{3.1}$$

$$w_{12} = w_{21} = {}_{.3} = w_{31} = u_{12} \ , \tag{3.2}$$

$$w_{22} = w_{33} = u_{22} + s_{22} \ , \tag{3.3}$$

$$w_{23} = w_{32} = u_{22} \ , \tag{3.4}$$

with s_{22} denoting the symmetry potential for a system of electrons with parallel spins at a density of ρ_2, which diverges logarithmically at the origin.[30] We now simplify notation by dropping the subscripts from s_{22} and defining

$$\rho = \rho_1 = 2\rho_2 = 2\rho_3 \ , \tag{3.5}$$

$$v = v_{11} = v_{22} = -v_{12} \ , \tag{3.6}$$

$$\epsilon = \epsilon_2 = \epsilon_1/\delta, \quad \delta = m_2/m_1 \ . \tag{3.7}$$

We then obtain the equations for the Fourier transforms of the three diffraction effective potentials, from Eq. (2.25):

$$\frac{\partial\tilde{u}_{11}}{\partial\beta} = \tilde{v} - \delta\epsilon\tilde{u}_{11} - \tilde{Q}_{11} - \tfrac{1}{2}\delta\rho\epsilon\tilde{u}_{11}^2 - \tfrac{1}{2}\rho\epsilon\tilde{u}_{12}^2 + \tilde{y}_{11} \ , \tag{3.8}$$

$$\frac{\partial\tilde{u}_{12}}{\partial\beta} = -\tilde{v} - \tfrac{1}{2}(1+\delta)\epsilon\tilde{u}_{12} - \tilde{Q}_{12} + \tilde{y}_{12} - \tfrac{1}{2}\delta\rho\epsilon\tilde{u}_{12}\tilde{u}_{11} - \tfrac{1}{2}\rho\epsilon\tilde{u}_{12}(\tilde{u}_{22} + \tfrac{1}{2}\tilde{s}) \ , \tag{3.9}$$

$$\frac{\partial\tilde{u}_{22}}{\partial\beta} = \tilde{v} - \tfrac{1}{2}\epsilon\tilde{u}_{22} - \tilde{Q}_{22} - \tfrac{1}{2}\delta\rho\epsilon\tilde{u}_{12}^2 - \tfrac{1}{2}\rho\epsilon\tilde{u}_{22}(\tilde{u}_{22} + \tilde{s}) + \tilde{y}_{22} \ . \tag{3.10}$$

Equations (3.8)–(3.10) were solved numerically using the boundary conditions indicated by Eq. (1.8):

$$\tilde{u}_{\mu\nu} \xrightarrow{\beta\to 0} 4\pi\beta Z_\mu Z_\nu e^2/x^2 \ , \tag{3.11}$$

where $\tilde{u}$ is defined in Eq. (2.28).

Let us first examine some limiting cases of the effective potentials. First, because of the boundary conditions on the diffraction potentials and the fact that the symmetry potential becomes negligible at high temperatures, the total effective potentials go over to the classical result at high temperatures. Second, at sufficiently high densities and low temperatures, Q and y become negligibly small and $\partial\tilde{u}_{\mu\nu}/\partial\beta$ goes to zero as the ground state is approached. Then the equations for the effective potentials are the same as those obtained by Allen and Dunn[31] using a variational calculation.

For finite temperatures and very low densities, those terms explicitly containing ρ may be neglected and the equations decouple. We may then compare these "zero"-density results with those obtained by Barker.[22] Barker directly performed the summation in Eq. (1.1) for a two-particle system. This comparison is illustrated in Figs. 1–3. The proton-electron effective potential is the most important one, and here the agreement is most striking. Figures 1 and 2 also show the result of neglecting y in Eq. (3.9), as was done in Ref. 25. It is seen that while y is not an extremely large term, including it greatly improves the results. The proton-proton effective potential, which is not illustrated, is essentially identical to Barker's result, except for small deviations at distances less than 0.5 Bohr radii. There are several features of importance in these effective potentials. They are all asymptotic to $\pm\beta e^2/r$. As expected, the divergence of the Coulomb potential at the origin has been eliminated; this is due to the tunnel effect. The extended linear behavior of the proton-electron effective potential at small radii is quite striking. An explanation for this is readily obtainable. If one retains only the ground-state energy eigenfunction in the two-particle Slater sum, one gets

$$W^{(2)} \simeq (c/\pi) e^{-2r/a_0 - \beta E_0} , \tag{3.12}$$

or

$$u_{12}^{(2)} = -\ln W^{(2)} \simeq \beta E_0 + 2r/a_0 + \ln(\pi/c) , \tag{3.13}$$

where E_0 is -1 Ry and a_0 is the Bohr radius. This not only gives the correct slope of u_{12}, but also explains part of the temperature dependence of the value of u_{12} at the origin. It can easily be shown that for all densities, u_{12} will have the correct slope at the origin. Assume that

$$u_{12} \longrightarrow (\text{const}) + br. \quad \text{as } r \to 0 . \tag{3.14}$$

Then, we have

$$\tilde{u}_{12}(x) \sim -8\pi b/x^4 . \tag{3.15}$$

Only the first two terms in the right-hand side

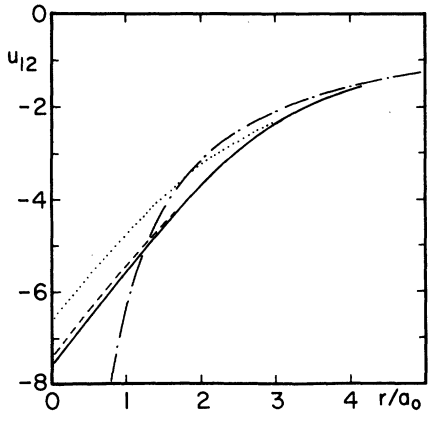

FIG. 1. Zero-density proton-electron effective potentials at $T = 5\times10^4$ °K. Solid line, Barker (Ref. 22); dash-dot line, Coulomb; dashed line, present calculation including y; dotted line, present calculation, neglecting y.

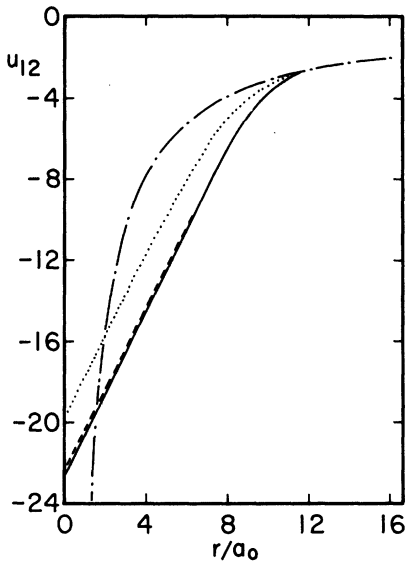

FIG. 2. Zero-density proton-electron effective potentials at $T = 1\times10^4$ °K. Solid line, Barker (Ref. 22); dash-dot line, Coulomb; dashed line, present calculation including y; dotted line, present calculation, neglecting y.

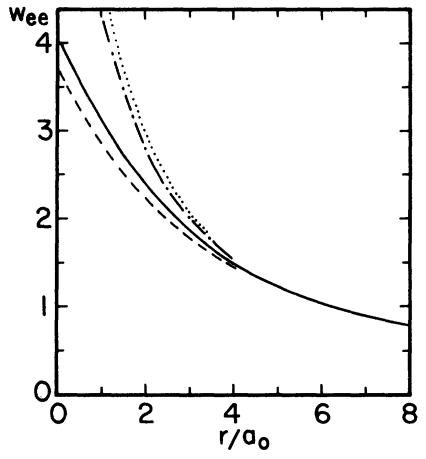

FIG. 3. Zero-density electron-electron total effective potentials at $T = 5\times10^4$ °K. Solid line, Barker (Ref. 22) for antiparallel-spin electrons; dashed line, present calculation for antiparallel-spin electrons; dash-dot line, Barker for parallel-spin electrons; dotted line, present calculation for parallel-spin electrons.

(RHS) of Eq. (3.9) contribute to order $1/x^2$ at large x. They are

$$-4\pi e^2/x^2+\tfrac{1}{2}(1+\delta)(\hbar^2/2m_2)(8\pi b/x^2)=0 \qquad (3.16)$$

or

$$b=\frac{2m_2e^2}{\hbar^2(1+\delta)}=2/a_0 \ . \qquad (3.17)$$

The large-r behavior of the effective potentials at all densities can also be easily obtained from the differential equations. Assume that for large r

$$u_{\mu\nu}(r)\sim\pm e^2/kT'r \ , \qquad (3.18)$$

where T' is an effective temperature which is a function of both temperature and density. Then we have

$$\tilde{u}_{\mu\nu}(x)\xrightarrow[x\to 0]{}\pm 4\pi e^2/kT'x^2 \ . \qquad (3.19)$$

Only the partial derivative with respect to β, $\tilde{v}$, and the terms explicitly containing the density, contribute to order $1/x^2$ at small x in Eq. (3.9). It is then easy to show that

$$kT'=a\coth\beta a \ , \qquad (3.20)$$

where

$$a=\tfrac{1}{2}(1+\delta)^{1/2}\hbar\omega_{pl} \ , \qquad (3.21)$$

and ω_{pl} is the plasma frequency of an electron gas at this density:

$$\omega_{pl}=(4\pi\rho e^2/m_2)^{1/2} \ . \qquad (3.22)$$

It may be noted that

$$T'\to T \quad \text{as } T\to\infty \ , \qquad (3.23)$$

$$kT'\to\tfrac{1}{2}(1+\delta)^{1/2}\hbar\omega_{pl} \quad \text{as } T\to 0 \ . \qquad (3.24)$$

The density dependence of the numerical solutions of Eqs. (3.8)–(3.10) for the boundary condition in Eq. (3.11) is illustrated in Fig. 4. The main feature is that the effective potentials become weaker, and go over to their asymptotic form sooner, as the density increases. Also, the "zero"-density limit, in which Barker's two-particle effective potentials are valid, is seen to correspond to a fairly high density, about 6×10^{20} electrons/cm^3 at $T=4.31\times10^4$ °K. This density is a function of temperature, increasing as the temperature decreases. The condition for no density effects at large radii may be obtained by requiring $T'\simeq T$ in Eq. (3.20). This condition appears to be well approximated by

$$\log_{10}\rho\lesssim 2\log_{10}T+11.5 \ , \qquad (3.25)$$

where ρ is in electrons/cm^3 and T is in °K.

Some sample values of the effective potentials are given in Tables I–IV.

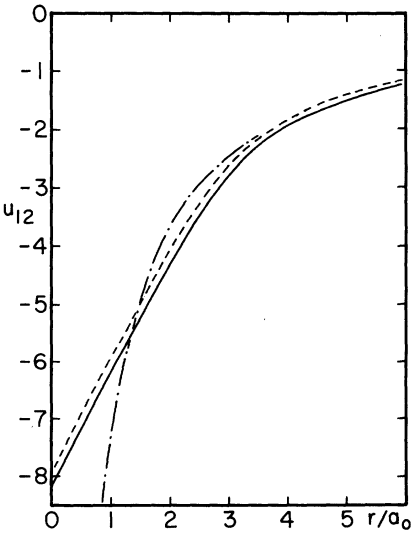

FIG. 4. Density dependence of proton-electron effective potential at $T=4.31\times10^4$ °K. Solid line, $\rho=1\times10^{18}$ electrons/cm^3; dashed line, $\rho=6.76\times10^{21}$ electrons/cm^3; dash-dot line, Coulomb, $\beta e^2/r$.

IV. RESULTS

In this section, results will be presented for the distribution of particles in a system of partially ionized hydrogen, using the effective potentials. The pair correlation function between particles of types μ and ν is defined by

$$g_{\mu\nu}(r_{12})=\left(1-\frac{\delta_{\mu\nu}}{N_\mu}\right)\Omega^2\frac{\int e^{-B}\,d\vec{r}_3\cdots d\vec{r}_N}{\int e^{-B}d\vec{r}_1\cdots d\vec{r}_N} \ , \qquad (4.1)$$

TABLE I. Proton-electron effective potentials at a density of 6.76×10^{21} electrons/cm^3.

	T (°K)			
$r/(0.3107a_0)$	4.31×10^4	5.09×10^4	8.00×10^4	1.12×10^5
0	−7.90	−7.16	−5.43	−4.38
1	−7.29	−6.55	−4.87	−3.87
2	−6.68	−5.95	−4.29	−3.32
3	−6.08	−5.36	−3.74	−2.81
4	−5.49	−4.78	−3.21	−2.34
5	−4.91	−4.21	−2.72	−1.93
6	−4.34	−3.67	−2.28	−1.59
7	−3.81	−3.18	−1.91	−1.32
8	−3.32	−2.73	−1.62	−1.12
10	−2.50	−2.05	−1.24	−0.87
12	−1.96	−1.63	−1.02	−0.73
14	−1.64	−1.39	−0.89	−0.64
16	−1.43	−1.22	−0.78	−0.56
20	−1.13	−0.97	−0.63	−0.45
24	−0.94	−0.80	−0.52	−0.38
28	−0.80	−0.69	−0.45	−0.32
32	−0.70	−0.60	−0.39	−0.28

TABLE II. Proton-proton effective potentials at a density of 6.76×10^{21} electrons/cm^3.

	T (°K)			
$r/(0.3107a_0)$	4.31×10^4	5.09×10^4	8.00×10^4	1.12×10^5
0	124.1	119.5	106.2	95.0
1	22.18	19.21	12.84	9.44
2	11.34	9.70	6.27	4.51
3	7.51	6.44	4.17	3.00
4	5.59	4.80	3.12	2.25
5	4.45	3.83	2.50	1.80
6	3.69	3.18	2.08	1.50
7	3.16	2.73	1.78	1.28
8	2.77	2.39	1.56	1.12
10	2.22	1.91	1.25	0.90
12	1.86	1.60	1.04	0.75
14	1.59	1.37	0.89	0.64
16	1.39	1.20	0.78	0.56
20	1.12	0.96	0.62	0.45
24	0.93	0.80	0.52	0.37
28	0.80	0.69	0.45	0.32
32	0.70	0.60	0.39	0.28

where particle 1 is of type μ, particle 2 is of type ν, and Ω is the volume of the system. In Ref. 25 the hypernetted chain integral equation[29] was used to obtain the correlation functions, but this method proved to be inadequate. Hence, a Monte Carlo method was employed here. Because of the long-range nature of the effective pair potentials, it was necessary to use the Ewald[32] sum for including the effects of the long-range interactions. We used a MC method developed by Barker[28]; it is essentially an extension of the one-component

TABLE III. Electron-electron diffraction effective potentials at a density of 6.76×10^{21} electrons/cm^3.

	T (°K)			
$r/(0.3107a_0)$	4.31×10^4	5.09×10^4	8.00×10^4	1.12×10^5
0	3.85	3.59	2.95	2.53
1	3.55	3.30	2.65	2.24
2	3.29	3.03	2.40	1.98
3	3.05	2.80	2.17	1.76
4	2.83	2.58	1.97	1.57
5	2.63	2.39	1.79	1.41
6	2.45	2.21	1.63	1.27
7	2.29	2.06	1.49	1.14
8	2.13	1.91	1.37	1.04
10	1.88	1.67	1.16	0.86
12	1.66	1.46	1.00	0.73
14	1.48	1.29	0.87	0.64
16	1.33	1.16	0.77	0.56
20	1.09	0.94	0.62	0.45
24	0.92	0.79	0.52	0.37
28	0.79	0.68	0.45	0.32
32	0.69	0.60	0.39	0.28

TABLE IV. Total electron-electron effective potentials for electrons with parallel spins at a density of 6.76×10^{21} electrons/cm^3.

	T (°K)			
$r/(0.3107a_0)$	4.31×10^4	5.09×10^4	8.00×10^4	1.12×10^5
0	∞	∞	∞	∞
1	7.88	7.45	6.36	5.61
2	6.25	5.83	4.77	4.04
3	5.23	4.82	3.79	3.09
4	4.48	4.09	3.09	2.44
5	3.90	3.51	2.57	1.96
6	3.42	3.05	2.16	1.61
7	3.02	2.68	1.85	1.35
8	2.70	2.37	1.60	1.15
10	2.18	1.90	1.25	0.90
12	1.82	1.57	1.03	0.74
14	1.56	1.34	0.88	0.64
16	1.36	1.17	0.77	0.56
20	1.10	0.95	0.62	0.45
24	0.92	0.79	0.52	0.37
28	0.79	0.68	0.45	0.32
32	0.69	0.60	0.39	0.28

method used by Brush, Sahlin, and Teller[27] for the classical electron gas. The pair correlation functions were obtained from

$$g_{\mu\nu}(r)=\bar{N}_{\mu\nu}(r-\tfrac{1}{2}\Delta r;\ r+\tfrac{1}{2}\Delta r)/(4\pi\rho_\nu r^2\Delta r)\ , \tag{4.2}$$

where $\bar{N}_{\mu\nu}$ is the average number of particles of type ν counted in a spherical shell about a particle of type μ.

The basic cell contained 60 particles: 30 protons, 15 electrons with spin-up, and 15 electrons with spin-down. A mesh of 1000 points across the basic cell in each direction was used. As few as 90 000 and as many as 330 000 attempted moves were generated for each run, with the first 30 000 thrown out. It was possible to discard relatively few moves because the final configuration from the previous temperature was used for the initial configuration with relatively small steps in temperature, so that each run was started close to equilibrium. Up to 1 000 000 moves were used in runs made to check the accuracy of the procedure.

Figures 5 and 6 illustrate the temperature dependence of the parallel- and antiparallel-spin electron distributions $P_{\mu\nu}(r)=4\pi\rho_\mu r^2 g_{\mu\nu}(r)$ at a density of 6.00×10^{20} electrons/cm^3. $P(r)$ gives the probability of finding a particular particle in a spherical shell of radius r about a given particle. The Fermi hole in the parallel spin case is clearly visible; it is caused by the symmetry effective potential which diverges as $-2\ln r$ at the origin. The peaks in P_{23} at the lower temperatures are evidently caused by the presence of a few nega-

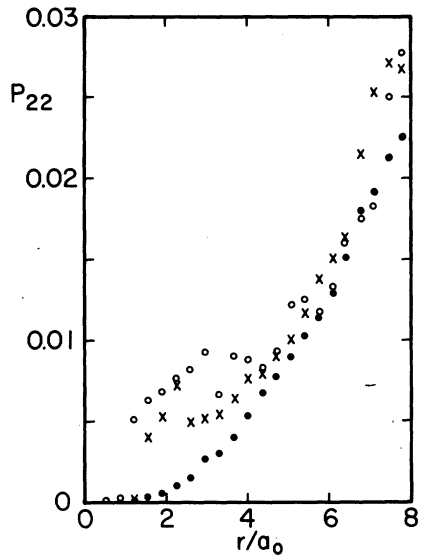

FIG. 5. Temperature dependence of parallel-spin electron distribution $P_{22}=4\pi\rho_2 r^2 g_{22}$ at $\rho=6\times10^{20}$ electrons/cm^3. Fifteen-point smoothing was used on the original Monte Carlo data. Every fifth point is plotted. Solid circles, $T=5.09\times10^4$ °K; ×'s, $T=3.73\times10^4$ °K; open circles, $T=3.29\times10^4$ °K.

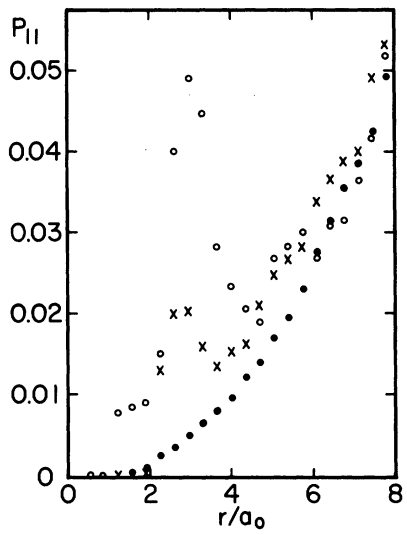

FIG. 7. Temperature dependence of proton-proton distribution $P_{11}=4\pi\rho r^2 g_{11}$ at $\rho=6\times10^{20}$ electrons/cm^3. Fifteen-point smoothing was used on the original Monte Carlo data. Every fifth point is plotted. Solid circles, $T=5.09\times10^4$ °K; ×'s, $T=3.73\times10^4$ °K; open circles, $T=3.29\times10^4$ °K.

tive ions in the system. The temperature dependence of the proton-proton distribution is shown in Fig. 7. The peaks at the lower temperatures are possibly caused by a few H_2 molecules and H_2^+ ions. The primary feature of the proton-electron correlation function is a large peak at the origin which grows as the temperature is lowered. Since a plot of this peak would be uninformative, we have plotted P_{12} in Fig. 8. The trend is for the peak to rise as the temperature declines; the position of the peak increases from $1a_0$ as the

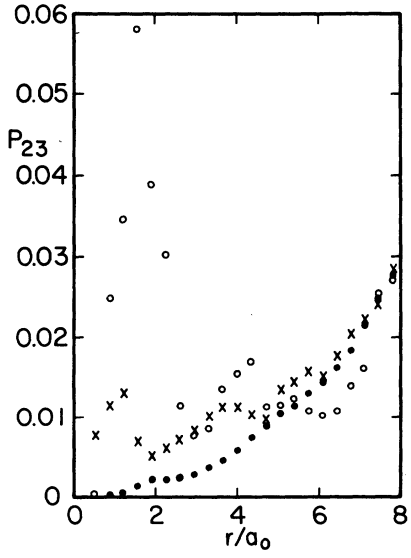

FIG. 6. Temperature dependence of antiparallel-spin electron-electron distribution $P_{23}=4\pi\rho_2 r^2 g_{23}$ at $\rho=6\times10^{20}$ electrons/cm^3. Fifteen-point smoothing was used on the original Monte Carlo data. Every fifth point is plotted. Solid circles, $T=5.09\times10^4$ °K; ×'s, $T=3.73\times10^4$ °K; open circles, $T=3.29\times10^4$ °K.

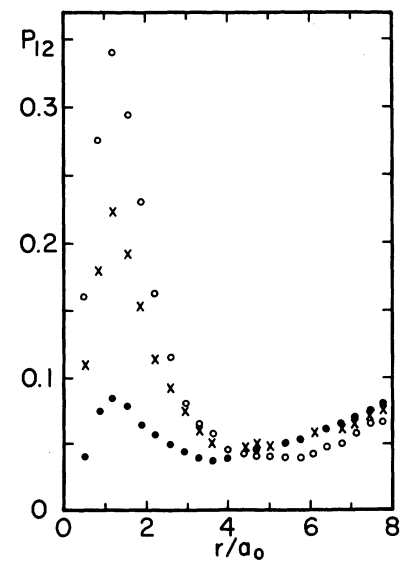

FIG. 8. Temperature dependence of proton-electron distribution $P_{12}=4\pi\rho r^2 g_{12}$ at $\rho=6\times10^{20}$ electrons/cm^3. Fifteen-point smoothing was used on the original Monte Carlo data. Every fifth point is plotted. Solid circles, $T=5.09\times10^4$ °K; ×'s, $T=3.73\times10^4$ °K; open circles, $T=3.29\times10^4$ °K.

temperature increases. This function for an isolated atom in the ground state would be, at small distances, proportional to r^2e^{-2r/a_0}, which, of course, has a peak at $1a_0$. Thus, as the temperature decreases and more atoms are found, one would expect $P_{12}(r)$ to increase as it does.

The density dependence of the correlations are shown in Figs. 9–13. The radial excess $4\pi\rho r^2(g_{12}-1)$, plotted in Fig. 13, has the uniform probability subtracted out. It emphasizes that for a given temperature, the number of atoms increases as the density increases. Of course, if we had gone to sufficiently high densities, pressure ionization would have terminated this trend.

While the results illustrated in this section are all quite reasonable, very unreasonable results were obtained when MC calculations were done at lower temperatures than those illustrated: all the particles in the MC base cell formed a cluster which might be interpreted as an H_{32} molecule. While the effective potentials appear to be reasonable, it must be remembered that the forces between molecules are in a very delicate balance due to the cancellation of all the Coulomb forces. Hence, a small error in the pair effective potentials could be causing this problem; there is much room for improvement in the reduction of Eq. (2.17) to Eq. (2.25). On the other hand, this could

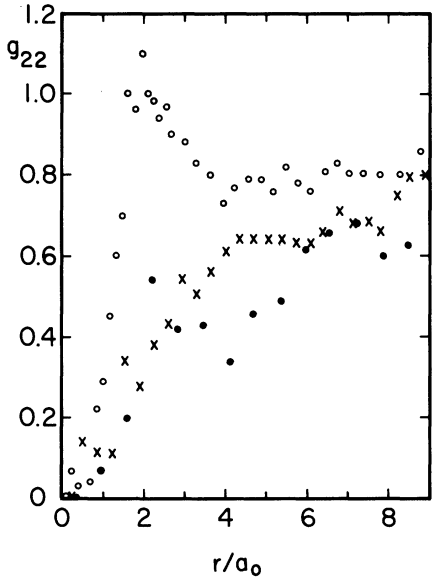

FIG. 9. Density dependence of parallel-spin electron-electron pair correlation function at $T=5.09\times10^4$ °K. Fifteen-point smoothing was used on the original Monte Carlo data. Every fifth point is plotted except at large r, where some points have been omitted for clarity. Solid circles, $\rho=1.00\times10^{20}$ electrons/cm^3; ×'s, $\rho=6.00\times10^{20}$ electrons/cm^3; open cirlces, $\rho=6.76\times10^{21}$ electrons/cm^3.

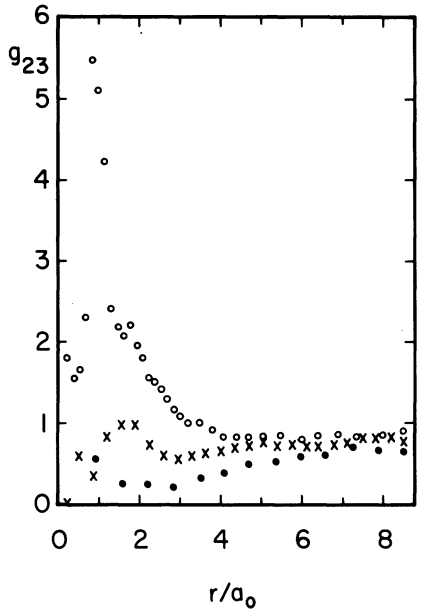

FIG. 10. Density dependence of antiparallel-spin electron-electron pair correlation function at $T=5.09\times10^4$ °K. Fifteen-point smoothing was used on the original Monte Carlo data. Every fifth point is plotted except at large r, where some points have been omitted for clarity. Solid circles, $\rho=1.00\times10^{20}$ electrons/cm^3; ×'s, $\rho=6.00\times10^{20}$ electrons/cm^3; open circles, $\rho=6.76\times10^{21}$ electrons/cm^3.

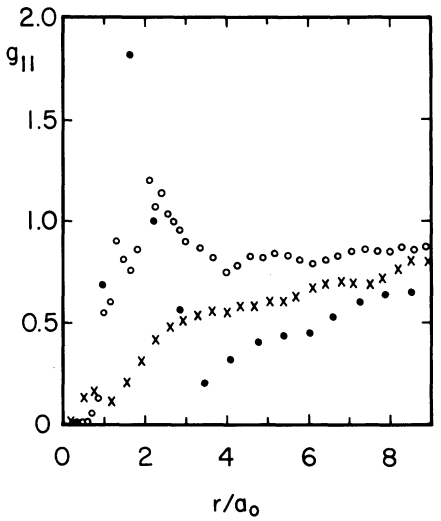

FIG. 11. Density dependence of proton-proton pair correlation function at $T=5.09\times10^4$ °K. Fifteen-point smoothing was used on the original Monte Carlo data. Every fifth point is plotted except at large r, where some points have been omitted for clarity. Solid circles, $\rho=1.00\times10^{20}$ electrons/cm^3; ×'s, $\rho=6.00\times10^{20}$ electrons/cm^3; open circles, $\rho=6.76\times10^{21}$ electrons/cm^3.

well be indicating that the pair approximation is no longer adequate when there are molecules present; three- or four-body effective potentials might have to be included.

From Fig. 8, and the discussion about it, the idea arises that from the proton-electron correlation function and our knowledge of the wave function for the ground state of an isolated atom, one should be able to ascertain the fraction of particles in the ground state of an atom. Indeed, it is possible to do this. The method for obtaining this information from the MC data is derived in Appendix B. Figure 14 compares our results with those of Patch,[33] who employed the known isolated atom energies. It was necessary to interpolate from Patch's tables to obtain the desired numbers. Figure 14 shows that at low densities, we are in good agreement with Patch. The highest density shown illustrates the potential value of the present technique; Patch could not obtain results at this density primarily because of polarization of the atoms. However, the MC calculation used here handles this problem very easily and naturally. Our results for the fraction of particles not in the ground state of an atom may be summarized by the fitted formula

$$f = \tfrac{1}{2}[1 + \mathrm{erf}(b \ln T/T_0)] \ , \qquad (4.3)$$

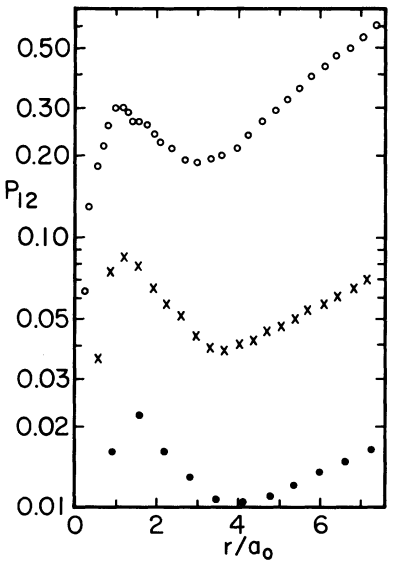

FIG. 12. Density dependence of proton-electron distribution $P_{12} = 4\pi\rho r^2 g_{12}$ at $T = 5.09 \times 10^4$ °K. Fifteen-point smoothing was used on the original Monte Carlo data. Every fifth point is plotted except at large r, where some points have been omitted for clarity. Solid circles, $\rho = 1.00 \times 10^{20}$ electrons/cm^3; ×'s, $\rho = 6.00 \times 10^{20}$ electrons/cm^3; open circles, $\rho = 6.76 \times 10^{21}$ electrons/cm^3.

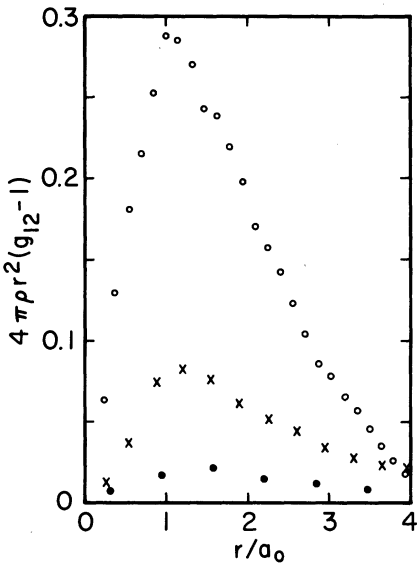

FIG. 13. Density dependence of proton-electron radial excess $4\pi\rho r^2(g_{12} - 1)$ at $T = 5.09 \times 10^4$ °K. Fifteen-point smoothing was used on the original Monte Carlo data. Every fifth point is plotted except at large r, where some points have been omitted for clarity. Solid cirlces, $\rho = 1.00 \times 10^{20}$ electrons/cm^3; ×'s, $\rho = 6.00 \times 10^{20}$ electrons/cm^3; open circles, $\rho = 6.76 \times 10^{21}$ electrons/cm^3.

where

$$T_0 = 10^5 \text{ °K}/(24.62 - 1.04 \log_{10}\rho) \ , \qquad (4.4)$$

$$b = 14.35 - 0.61 \log_{10}\rho \ , \qquad (4.5)$$

and ρ is measured in electrons/cm^3.

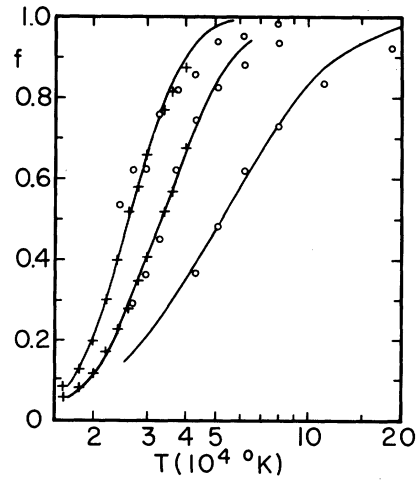

FIG. 14. Fraction of particles not in the ground state of an atom as a function of temperature and density. Solid line, fitted function, Eq. (4.3); +'s, interpolated from Patch (Ref. 33); 0's, present calculation. The densities plotted are, from left to right, $\rho = 1.00 \times 10^{20}$, 6.00×10^{20}, 6.76×10^{21} electrons/cm^3.

V. CONCLUSIONS

The Slater sum has been approximated in the form of a classical Boltzmann factor with the Coulomb potential replaced by effective potentials. The differential equation resulting from differentiating the Slater sum with respect to β, Eq. (2.17), has been broken into a part which can be expressed as sums of effective potentials, and a part $Y - Y_I$ which contains a sum over eigenfunctions of the system and which has been shown to be well approximated by a modified Thomas-Fermi method. This equation was reduced to a differential equation for pair effective potentials, Eq. (2.25), and was solved numerically. Pair-distribution functions, computed from these effective potentials by a Monte Carlo calculation, appear to be reasonable. The Fermi hole is clearly visible in the parallel-spin electron-electron correlation function. The proton-electron radial excess $4\pi\rho r^2$ $(g_{12} - 1)$ increases as the temperature is lowered, and has a peak near $1a_0$, as expected. The proton-proton and antiparallel-spin electron-electron pair correlation functions provide evidence that some H^- and H_2^+ ions may have formed at the lowest temperatures. In spite of the excellent agreement of the pair effective potentials with Barker's results at low density and with Allen and Dunn's results at high density and low temperature, the failure of the procedure when fewer than 40% of the atoms are ionized seems to indicate that either three-body effective potentials must be considered or that the pair effective potentials must be calculated more accurately. The excellent agreement with Patch's results for the fraction of particles in the ground state of an atom, and the ability to extend these calculations to higher density, indicates that the present procedure does have considerable merit.

A method with fewer approximations and with the capability of including three-body effective potentials is currently being investigated.

ACKNOWLEDGMENTS

The authors wish to thank Dr. A. A. Barker, who wrote the initial version of the Monte Carlo program, Dr. R. L. Coldwell, who read and suggested improvements in the manuscript, and Randall J. Miller and Thomas O'Kuma, who assisted in the numerical computations. They also gratefully acknowledge the generous amounts of computing time made available by the Louisiana Tech University computing center.

APPENDIX A

In Sec. II it was found to be imperative to express $(Y - Y_I)$ as a sum of pair functions in order to obtain equations for the pair effective potentials. In this appendix, a method for doing this will be presented. The basic idea is to replace $(Y - Y_I)$ by a sum of pair functions y_{ij} that are the equivalent functions for a two-particle system with an average potential that contains the effects of the rest of the particles in the system replacing the Coulomb potential. We believe this to be a sort of Born-Oppenheimer[34] approximation, but are unable to prove this. We will treat a proton-electron pair first. Since $Y_I = 0$ here, we have

$$y_{ij} \simeq X^{(2)}/W^{(2)} - 3/2\beta - \tfrac{1}{4}\nabla u^{(2)} \cdot \nabla u^{(2)}, \tag{A1}$$

where

$$W^{(2)} = c \sum_{n,l,m} \psi^*_{n,l,m} e^{-\beta E_n} \psi_{n,l,m} \tag{A2}$$

and

$$X^{(2)} = c \sum_{n,l,m} e^{-\beta E_n} \nabla\psi^*_{n,l,m} \cdot \nabla\psi_{n,l,m} \tag{A3}$$

In this Appendix, n denotes the principle quantum number, and we have defined $\alpha = (1 + \delta)a_e$.

The procedure will be used to determine ψ_{nlm} and E_n from the average potential, to evaluate $W^{(2)}$ and $X^{(2)}$, to obtain $u^{(2)}$ from

$$u^{(2)} = -\ln W^{(2)}, \tag{A4}$$

and to insert the results into Eq. (A1) to obtain y_{ij}. Henceforth, the superscripts indicating that the quantities are for a two-particle system will be dropped, as only two-body quantities are considered in this appendix.

The first problem is finding an expression for the average potential. Clearly, it must be Coulomb at small distances and must go to zero at large distances due to shielding by the other particles. We will assume it to be a truncated Coulomb potential which is zero beyond the ion-sphere radius r_s. Using Bohr units, the average potential is

$$\begin{aligned} v(r) &= -2/r + 2/r_s, \quad r \leq r_s \\ &= 0, \quad r > r_s. \end{aligned} \tag{A5}$$

In principle, one could obtain all of the ψ_{nlm}'s and perform the summation (integration for the continuous states) by a procedure similar to Barker's. However, since y is a small term in the equation for the effective potentials, we are willing to sacrifice some accuracy for the sake of simplicity. One simple method would be to use the Thomas-Fermi approximation (TFA).[35,36] Unfortunately, the TFA is not a good approximation for hydrogen. Hence, we will use a modified form of the TFA which treats the ground state of the atom separately; this method proves to be quite good.

In this approximation, the radial part of the wave function is given by[36]

$$R_{nl}=\frac{1}{Arp^{1/2}}\cos\left(\int_r^{r_2} p\,dr-\frac{\pi}{4}\right),\quad r_1<r<r_2$$
$$=0,\quad r\le r_1,\ r\ge r_2, \tag{A6}$$

where r_1 and r_2 are the classical turning points and

$$p^2=E-v_l(r)\ , \tag{A7}$$
$$v_l(r)=v(r)+(l+\tfrac{1}{2})^2/r^2\ , \tag{A8}$$
$$A^2=4\pi\int_{r_1}^{r_2} p^{-1}\,dr\ . \tag{A9}$$

The function p is restricted by the condition

$$\int_{r_1}^{r_2} p\,dr=(n+l+\tfrac{1}{2})\pi\ , \tag{A10}$$

implying that

$$\frac{dn}{dE}=\frac{A^2}{8\pi^2}\ . \tag{A11}$$

Inserting the wave function into the Slater sum and replacing $\cos^2$ by its average, $\frac{1}{2}$, we obtain

$$W=\frac{(4\pi\beta)^{3/2}}{r^2}\sum_n\sum_l\frac{2l+1}{A^2p}e^{-\beta E}\chi(p^2)\ , \tag{A12}$$

where χ is defined by

$$\chi(x)=1,\quad x>0$$
$$=0,\quad x\le 0\ . \tag{A13}$$

The summations will now be converted to integrals.

$$\sum_{l=0}^{\infty}\to\int_{-1/2}^{\infty}dl\ , \tag{A14}$$

$$\sum_{n=1}^{\infty}\to\int_{1/2}^{\infty}dn=\int_{E_c}^{\infty}\frac{A^2}{8\pi^2}dE\ , \tag{A15}$$

where we have used Eq. (A11). If we wished to sum over all states, E_c would be taken to be negative infinity. However, since that procedure gives poor results, W will be calculated as a ground-state term plus a restricted sum which contains the remaining states:

$$W=W_G+W_R\ . \tag{A16}$$

If the ion-sphere radius is sufficiently large, the ground-state wave function may be approximated by that of an isolated atom:

$$\psi_G\approx\pi^{-1/2}e^{-r} \tag{A17}$$

and the energy will merely be shifted by a constant from the strict Coulomb case

$$E_n=-1/n^2+2/r_s\ . \tag{A18}$$

Since we want to exclude $n=1$ from the sum in W_R, we take

$$E_c=E_{3/2}=-4/9+2/r_s\ . \tag{A19}$$

Thus, the TFA will be used for all the states except the ground state. Then we have

$$W_R=\frac{\pi^{-1/2}\beta^{3/2}}{r^2}\int_{E_c}^{\infty}dE\int_{-1/2}^{\infty}dl\,\frac{(2l+1)}{p}e^{-\beta E}\chi(p^2)\ . \tag{A20}$$

The result of doing the integrations is

$$W_R=e^{-\beta v}\operatorname{erfc}(\beta p_0)+(2\beta p_0/\sqrt{\pi})e^{-\beta E_c}\ , \tag{A21}$$

where

$$p_0^2=\max[0,E_c-v(r)]\ . \tag{A22}$$

From Eqs. (A17) and (A18), W_G is given by

$$W_G=8\pi^{1/2}\beta^{3/2}e^{-2r-E_1}\ , \tag{A23}$$

where

$$E_1=-1+(2/r_s)\ . \tag{A24}$$

We will calculate X in a similar manner. First, we easily find

$$X_G=W_G\ . \tag{A25}$$

In the spirit of the TFA, the Wentzel-Kramers-Brillouin (WKB) approximation to the gradient term in X_R will be used:

$$\nabla\Psi^*_{nlm}\cdot\nabla\Psi_{nlm}\simeq\Psi^*_{nlm}\Psi_{nlm}[E_n-v(r)]\ . \tag{A26}$$

In a manner analogous to that leading to Eq. (A20), we obtain

$$X_R=\int_{E_c}^{\infty}dE\int_{-1/2}^{\infty}dl\,\frac{(2l+1)\beta^{3/2}}{\sqrt{\pi}r^2}$$
$$\times[E-V_l(r)]^{-1/2}[E-V(r)]e^{-\beta E}\ . \tag{A27}$$

The final expression for X_R is easily shown to be

$$X_R=(3/2\beta)W_R+(2\beta^2p_0^3/\sqrt{\pi})e^{-\beta E_c}\ . \tag{A28}$$

The effective potential implied by this treatment is

$$u(r)=-\ln(W_G+W_R)\ . \tag{A29}$$

At very low densities, this function reproduces Barker's results as well as the effective potential obtained by integrating the differential equation (see Figs. 1 and 2).

The quantity y is obtained by inserting the results from Eqs. (A21), (A23), (A25), (A28), and (A29) into Eq. (A1).

We have also considered more complicated and realistic forms for the average potential, and

have solved the Schroedinger equation numerically to obtain the ground-state wave function and energy. Using the resulting y in the differential equation makes essentially no difference at the densities considered, although the results will be sensitive to the choice of the average potential if the density becomes sufficiently large.

For a two-electron or two-proton system, there is no dominant ground state, and the TFA can be used for the entire sum over states, implying $E_c = -\infty$. This gives

$$y_{11} = y_{22} = X/W - 3/2\beta = 0 \ . \tag{A30}$$

Since we feel that this should be the dominant term in y, it would appear to be best to neglect the other terms in y until a better approximation is developed for X and W in this case. Therefore, for the electron-electron and proton-proton equations, we will assume

$$y \simeq 0 \ , \tag{A31}$$

as was done in Ref. 25. As may be seen in Fig. 3, this approximation does not appear to cause great harm for low densities.

APPENDIX B

In this appendix, a method will be presented for obtaining the fraction of electrons which are in the ground state of an atom from the MC data. It will be applicable only when the temperature is sufficiently high that the number of molecules formed is negligible. Also, the density must be sufficiently low that the ground-state wave function of an atom is not substantially different from that of an isolated atom. Let $P(G)$ be the probability that a proton is part of an atom in the ground state; $P(i)$ equal the probability that a proton is part of an atom in the ith excited state; $P(F)$ equal the probability that a proton is not part of an atom; $P(R\,|\,G)$ be the conditional probability that an electron in the ground state of an atom is within a distance R of the proton; $P(R\,|\,i)$ be equal to the conditional probability that an electron in the ith excited state of an atom is within a distance R of the proton; $P(R\,|\,F)$ be the conditional probability that a free electron is within a distance R of a particular proton; and $P(R)$ equal the probability that a particular proton has at least one electron within a distance R.

The last quantity is obtained from the MC data. By the laws of probability, it is given by

$$P(R) = P(G)P(R\,|\,G) + P(F)P(R\,|\,F) + \sum_i P(i)P(R\,|\,i) \ . \tag{B1}$$

We will neglect the last term involving the excited states. These form a majority of the bound states only in a very small temperature range where there are few atoms. Using the ground-state wave function for a single isolated atom, we obtain

$$P(R\,|\,G) = \int_0^R |\psi_{1s}(r)|^2 \, d\vec{\mathbf{r}} = 1 - (1 + 2R + 2R^2)e^{-2R} \ , \tag{B2}$$

where R is measured in units of a_0. Under the simplifying assumption that the free electrons and protons are completely uncorrelated, $P(R\,|\,F)$ is given by the density of free electrons multiplied by the volume enclosed by a sphere of radius R (provided that $\rho\Delta V \ll 1$):

$$P(R\,|\,F) \simeq P(F)\rho\Delta V \ . \tag{B3}$$

Using $P(F) = 1 - P(G)$, we then obtain

$$P(G)P(R\,|\,G) + [1 - P(G)]^2\rho\Delta V - P(R) = 0 \ . \tag{B4}$$

Solving Eq. (B4) for $P(G)$, we obtain

$$P(G) = \left(2\rho\Delta V - P(R\,|\,G) + \{P^2(R\,|\,G) + 4\rho\Delta V[P(R) - P(R\,|\,G)]\}^{1/2}\right) \Big/ 2\rho\Delta V \ . \tag{B5}$$

Note that if $P(G)$ is nearly unity, then

$$P(G) \simeq P(R)/P(R\,|\,G) \ , \tag{B6}$$

in agreement with the intuitive result.

If this method is to be useful, then $P(G)$ must be relatively insensitive to R. If $P(G)$ is sensitive to the choice of R, then at least one of the approximations is breaking down. It is difficult to conceive of any of the approximations breaking down without causing $P(G)$ to be sensitive to the choice of R. Distances varying by a factor of 3 were used to determine the sensitivity. Typical results are given in Table V. The maximum difference here is 0.05. At the higher temperatures there is a trend for $P(G)$ to increase as R increases. This is probably due to the correlation of the large

TABLE V. Estimated fraction of particles in the ground state of an atom as a function of the radius chosen in Eq. (B5); $\rho = 6.76 \times 10^{21}$ electrons/cm^3, $R_1 = 1.025a_0$.

T (°K)	R_1	$2R_1$	$3R_1$	Mean
56.00×10^4	0.02	0.02	0.02	0.02
18.67×10^4	0.06	0.08	0.09	0.08
11.20×10^4	0.16	0.16	0.18	0.17
8.00×10^4	0.25	0.27	0.30	0.27
6.22×10^4	0.37	0.38	0.40	0.38
5.09×10^4	0.52	0.51	0.52	0.52
4.31×10^4	0.66	0.62	0.62	0.63

number of free particles which are present at the higher temperatures. In computing $P(G)$, which is used in Fig. 14, we have used the average of $P(G)$ calculated for the three radii (approximately $1a_0$, $2a_0$, and $3a_0$).

This method should be contrasted with the expedient of merely computing the fraction of electrons within a given distance (e.g., $2a_0$) of a proton and taking this to be the fraction of atoms present.

---

*Work supported in part by a grant from the National Science Foundation.

[1]G. E. Uhlenbeck and L. Gropper, Phys. Rev. 41, 79 (1932).
[2]G. E. Uhlenbeck and E. Beth, Physica (Utr.) 3, 726 (1936).
[3]J. G. Kirkwood, Phys. Rev. 44, 31 (1933).
[4]E. Meeron, J. Chem. Phys. 28, 630 (1958).
[5]T. Morita, Prog. Theor. Phys. 22, 757 (1959).
[6]R. Abe, Prog. Theor. Phys. 21, 421 (1959); 21, 941 (1959); 22, 213 (1959).
[7]G. Ecker and W. Kroll, Phys. Fluids 6, 62 (1963); Z. Naturforsch. 21a, 2012 (1966); 21a, 2023 (1966).
[8]R. Dekeyser, Physica (Utr.) 31, 1405 (1965).
[9]B. A. Trubnikov and K. F. Elesin, Zh. Eksp. Teor. Fiz. 47, 1279 (1964) [Sov. Phys.—JETP 20, 866 (1965)].
[10]W. Ebeling, Ann. Phys. (Leipz.) 19, 104 (1967).
[11]W. Ebeling, G. Kelbg, and R. Sandig, Beitr. Plasma Phys. 10, 507 (1970), and references therein.
[12]H. E. DeWitt, J. Math. Phys. 3, 1216 (1962); 7, 616 (1964).
[13]F. DelRio and H. E. DeWitt, Phys. Fluids 12, 791 (1969).
[14]F. Lado, J. Chem. Phys. 47, 5369 (1967).
[15]K. Matsuda, Phys. Fluids 11, 328 (1968).
[16]D. J. Mitchell and B. W. Ninham, Phys. Rev. 174, 280 (1968); M. D. Diesendorf and B. W. Ninham, J. Math. Phys. 9, 745 (1968).
[17]R. G. Storer, J. Math. Phys. 9, 964 (1968); Phys. Rev. 176, 326 (1968).
[18]B. Davies and R. G. Storer, Phys. Rev. 171, 150 (1968).
[19]V. S. Vorobev, G. E. Norman, and V. S. Filinov, Zh. Eksp. Teor. Fiz. 57, 838 (1969) [Sov. Phys.—JETP 30, 459 (1970)].
[20]A. A. Barker, Aust. J. Phys. 21, 121 (1968).
[21]A. A. Barker, Phys. Rev. 179, 129 (1969).
[22]A. A. Barker, J. Chem. Phys. 55, 1751 (1971).
[23]T. Dunn and A. A. Broyles, Phys. Rev. 157, 156 (1967); A. A. Broyles and T. Dunn, Int. J. Quantum Chem. Is, 803 (1967).
[24]R. W. Patch, J. Quant. Spectrosc. Radiat. Transfer 9, 63 (1969).
[25]A. A. Broyles, A. A. Barker, T. Dunn, and M. A. Pokrant, Int. J. Quantum Chem. IIIs, 293 (1969).
[26]N. Metropolis, A. W. Rosenbluth, M. N. Rosenbluth, A. H. Teller, and E. Teller, J. Chem. Phys. 21, 1087 (1953).
[27]S. G. Brush, H. L. Sahlin, and E. Teller, J. Chem. Phys. 45, 2102 (1966).
[28]A. A. Barker, Aust. J. Phys. 18, 119 (1965); Phys. Rev. 171, 186 (1968).
[29]J. M. J. van Leeuwen, J. Groeneveld, and J. de Boer, Physica (Utr.) 25, 792 (1959); E. Meeron, J. Math. Phys. 1, 192 (1960); Prog. Theor. Phys. 24, 588 (1960); T. Morita, *ibid.* 20, 920 (1958); 21, 361 (1959); 23, 175 (1960); 23, 829 (1960); T. Morita and K. Hiroike, *ibid.* 23, 385 (1960); 23, 1003 (1960); M. S. Green, Hughes Aircraft Co. Report, September 1959 (unpublished); L. Verlet, Nuovo Cimento 18, 77 (1960); G. S. Rushbrooke, Physica (Utr.) 26, 259 (1960).
[30]M. A. Pokrant and F. A. Stevens, Jr., J. Chem. Phys. 55, 5846 (1971).
[31]K. R. Allen and T. Dunn, Phys. Rev. 170, 293 (1968).
[32]P. P. Ewald, Ann. Phys. Leipz. 64, 253 (1921).
[33]R. W. Patch, NASA Technical Note TND-4993 (1969) (unpublished).
[34]M. Born and E. Oppenheimer, Ann. Phys. Leipz. 84, 457 (1927).
[35]J. S. Plaskett, Proc. R. Soc. Lond. A 66, 178 (1953).
[36]A. A. Broyles, Am. J. Phys. 29, 81 (1961).